

# SLURRY INFILTRATION TESTS FOR SLURRY SHIELD TUNNELLING IN SATURATED SAND

T. Xu

*Ghent University, Belgium*

A. Bezuijen

*Ghent University, Ghent, Belgium and Deltares, Delft, The Netherlands*

**ABSTRACT:** Tunnelling in saturated sand will cause excess pore pressures in the sand. This was the case during the construction of all tunnels in the Netherlands. This excess pore pressure influences the stability of the tunnel face. Therefore the magnitude of the excess pore pressure is of importance. Furthermore, it requires more information on the penetration process of the bentonite slurry as it will occur at the front of the tunnel face. This paper deals with preliminary infiltration tests to investigate some aspects of the infiltration. Results will be compared with theory.

## 1. INTRODUCTION

Excess pore pressures were measured in front of a slurry and EPB TBM (Broere, 2001; Bezuijen et al., 2001; Hoefsloot, 2001). In this paper it will be concentrated on slurry TBMs. It was shown by Broere and Bezuijen et al. that this excess pore pressure influences the stability of the tunnel face. This was used to construct the Green Hart Tunnel (Aime et al., 2003) and in the North/South line in Amsterdam (Kaalberg, 2013). In the design of this last tunnel it appeared that the properties of the slurry during infiltration are of importance. This initiated some new infiltration tests (Steeneken, 2016). However, theoretical work by Bezuijen & Steeneken (2016) showed that the infiltration velocity is much lower in front of a tunnel than in an infiltration test. Talmon et al. (2013) have shown that the maximum infiltration depth may depend on the infiltration velocity. They argue that the process of infiltration and external cake building depends on the Pecklet number. A lower penetration velocity may lead to a lower final penetration depth because the external filter cake build up will start earlier. The final penetration depth is of importance to know how stable the filter cake is during for example interventions under air pressure and how fast pore pressures built up after ring building when drilling starts again.

After a brief introduction in the theory, the paper describes the setup of the infiltration tests, the materials, the column infiltration apparatus and the preliminary tests are described. Next, the results from the laboratory tests are presented, followed by an overview of the limitations of the experiments and remarks. After that, different slurry infiltration formulas are fitted onto the results. The usability of the laboratory results as input for the groundwater flow models will be discussed.

## 2. THEORY

Different descriptions are used for the infiltration as a function of time. Well known is the formula suggested by Krause (1987):

$$x_t = \frac{t}{a+t} x_{\max} \quad (1)$$

where:  $x_t$  = the distance over which the slurry is infiltrated (m);  $t$  = the infiltration time;  $a$  = the time at which half the maximum infiltration distance is reached;  $x_{\max}$  = the maximum distance over which the slurry is infiltrated (m).

The maximum infiltration depth  $x_{\max}$  can be calculated by the following formula (Broere, 2001):

$$x_{\max} = \frac{\Delta p d_{10}}{\alpha \tau_y} \quad (2)$$

where:  $\Delta p$  = the excess pressure (Pa);  $d_{10}$  = the grain diameter for which 10% is finer than  $d_{10}$  (mm);  $\alpha$  = fitting factor ( $2 \leq \alpha \leq 4$ );  $\tau_y$  = yield strength of slurry (Pa).

The timespan  $a$  is determined by (Broere, 2001):

$$a = \frac{x_{\max}}{\frac{k}{n} \left[ \frac{\rho_w g x_{\max}}{\rho_w g x_{\max}} + \left( 1 + \frac{L_v}{L_s} \right) \sin(\theta) \right]} \quad (3)$$

where:  $k$  = the permeability of the saturated sand sample(m/s);  $n$  = the porosity of the sand (-);  $L_v$  = the total length of the column (m);  $L_s$  = the length of the sand column (m);  $\theta$  = 90 degrees, since the column stands vertical.

Writing this equation in terms of piezometric head, the pressure difference due to head difference can be skipped, leading to:

$$a = \frac{nL.L_z k \phi_0}{k \phi_0} \quad (4)$$

$\phi_0$  = the piezometric head at the infiltration front (m) and the  $x_{\max}$  as given Broere is replaced by  $L$  to be compatible with (Bezuijen et al. 2016).

The Eq. (1) is a purely empirical formula. It does not take into account the flow resistance of the sand for water and grout. Using the theory of Krause that the pressure drop over the infiltrated zone is linearly dependent with the thickness of the infiltrated zone, the progress of the infiltration zone can also be described using Darcy's law for the flow of the slurry and the water flow. For the situation of a tunnel this is presented by Bezuijen et al. (2016). For an infiltration column the formula reads:

The piezometric head in the soil just in front of the slurry and the piezometric head in the mixing chamber can be written as:

$$\phi_{mx} = \phi_0 + \frac{nv_p}{k_g} x + \frac{\phi_{mx}}{L} x \quad (5)$$

where:  $\phi_{mx}$  = the piezometric head at the boundary between the slurry and the sand (m);  $x$  = the distance over which the slurry is infiltrated (m);  $k_g$  = the permeability of the slurry through the pores (m/s);  $v_p$  = the pore velocity (m/s).

The flow in the sand in front of the slurry can be described according to Darcy's law as:

$$\phi_0 = \frac{nv_p}{k} (L_s - x) \quad (6)$$

Combination of (5) and (6) leads to the equation:

$$\frac{dx}{dt} = \frac{\phi_{mx} (1 - x/L)}{\left( \frac{n}{k} L_s + x.n \left( \frac{1}{k_g} - \frac{1}{k} \right) \right)} \quad (7)$$

This is a non-linear differential equation. The equation is solved with explicit numerical integration in a spreadsheet.

Talmon et al. (2013) have shown that the result of an infiltration test is determined by two processes. It starts with a mud spurt: the bentonite slurry penetrates into the soil the penetration velocity is relatively high. When the penetration slows down, the water flow in the bentonite slurry (thus the

water has a different velocity than the bentonite platelets) becomes of importance. Now, following a much lower discharge rate, an external filter cake is built. According to this last theory the results of an infiltration test can be plotted against the square root of time and this will result in an two different more or less straight lines, see Figure 1 (figure from Talmon et al. 2013). The line just after  $t=0$  (s) describes the mud spurt and the other line at larger values of  $t$ , the process of external filter cake built up. In the empirical formula of Krause this is implicitly included, but it will be shown that the formula is less accurate at larger values of  $t$ . In the formula based on Bezuijen & Steeneken this is not included. However, this is the only formula that takes into account the influence of the pore water flow which is of importance to extrapolate the results to the situation of a real tunnel.

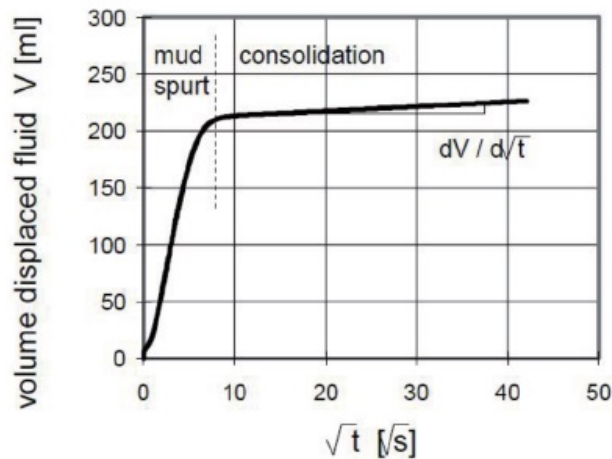


Figure 1: Volume of displaced fluid in time (Talmon et al., 2013).

### 3. TESTS PERFORMED

#### 3.1. TEST APPARATUS

The infiltration apparatus and the measurement principle are shown in Figure 2. Slurry is placed upon a saturated sand column which is pressurized with air. The air pressure is approximately 25 kPa due to the limitations of the laboratory equipment. When the valve at the bottom of the column is closed no infiltration can occur, because water cannot flow out of the apparatus. The slurry infiltration process starts when the valve at the bottom of the apparatus is opened.

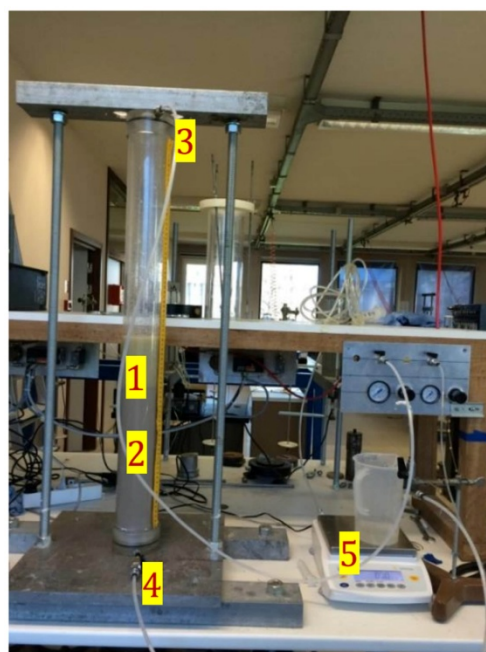


Figure 2: Infiltration apparatus and measurement system (1: slurry, 2: sand sample, 3: air pressure, 4: valve, 5: measurement system).

The weight of the discharged water from the column is measured with a balance. The measured value was stored in a computer 5 times per second. The measured value is the weight of the water that flows out from the bentonite. The whole process of test lasts about 30 minutes.

### 3.2. MATERIALS

In the laboratory experiments sieved sand M32 and IBECO B1 bentonite are used. The sieve curve of the sand used is shown in Figure 3. The bentonite used in the experiments is IBECO B1 which is the material used in the N/S line project in Amsterdam. To compile the slurry, 40, 50 and 60 grams of bentonite is added to 1 litre of water. The bentonite and water is mixed in a mixer and stiffened for 24 hours.

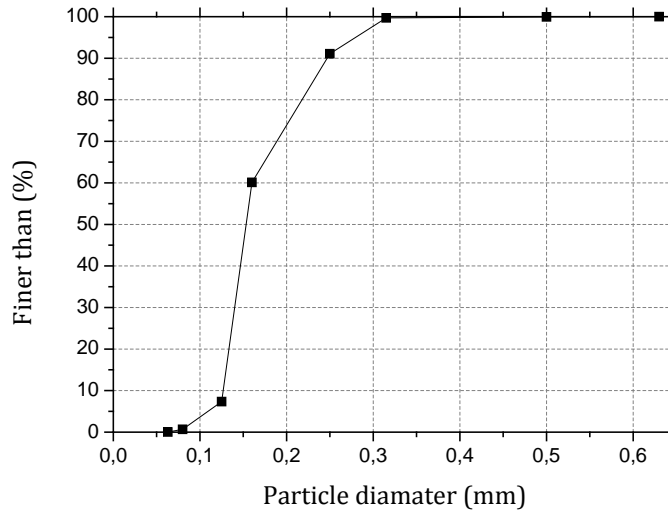


Figure 3: Sieve curve of the sand used in test.

### 3.3. PRELIMINARY TESTS

Prior to each column infiltration test three preliminary tests are performed to check whether the sand sample and the slurry are consistent. To check the consistency of the sand, the porosity and the permeability were measured. The porosity and the permeability of the sand are shown in Table 1. Also, every slurry mixture the yield point  $\tau_y$  is measured with a Fann viscometer. The details about the viscosity of the slurry are shown in Table 2. The formulas used in the preliminary tests can be found in Steeneken (2016).

Table 1: Properties of sand sample

Bentonite content	Column height	Porosity n	Permeability
g/L	cm	-	m/s
40	29.8	0.38	3.4E-4
50	28.5	0.38	3.6E-4
60	30	0.38	3.3E-4

Table 2: Properties of slurry used

Bentonite content	Yield point	Apparent Viscosit	$\tau_y$
g/L	Pa	cP = mPa*s	Pa
40	5.1	9.0	5.1
50	9.2	13.0	10.2
60	14.8	22.5	16.9

### 3.4. INFILTRATION TESTS

By opening the valve at the bottom of the column, the test starts. After 30 minutes, the valve is closed at the bottom and the air pressure on the top is released. The slurry is poured slowly onto the top of the

sand sample to avoid that the porosity and the permeability of the sand sample is affected by the pouring. A constant air pressure is important during infiltration, because the fluctuation of the air pressure may have a significant effect on the results.

## 4. RESULTS AND DISCUSSIONS

### 4.1. MEASURED RESULTS FROM THE INFILTRATION TESTS

For all the tests a change in gradient is clearly visible. The change in gradient implies the transition from slurry infiltration (mud spurt) to plastering (external filter cake formation) (Talmon et al., 2013). The x-axis in the graph is presented in  $\sqrt{t}$ , because this makes the change in the gradient easier to identify.

The measured volume of displaced fluid  $V_{pw}$  and parameters calculated by Eq. (2), (3) and (8) for each test are summarized in the Table 3. The measured displaced volumes in three tests are shown in Figure 4. It is seen that the discharged water volume decreases with the higher bentonite percent (from 40 to 60 g/L). The gradients of the lines in the mud spurt and consolidation areas are very different due to the different mechanisms, see the section about the theory. When using 60 g/L bentonite, the test result plotted against the square root of time results in lines for both the mud spurt and the consolidation areas that are nearly straight. In the tests using 40 g/L and 50 g/L bentonite, the lines during the mud spurt area are straight, while the lines in the consolidation area are not straight, again plotted against square root of time. This means that the external consolidation process cannot be described with linear consolidation theory. Likely it is caused by the large density increase of the slurry when it consolidates to a filter cake.

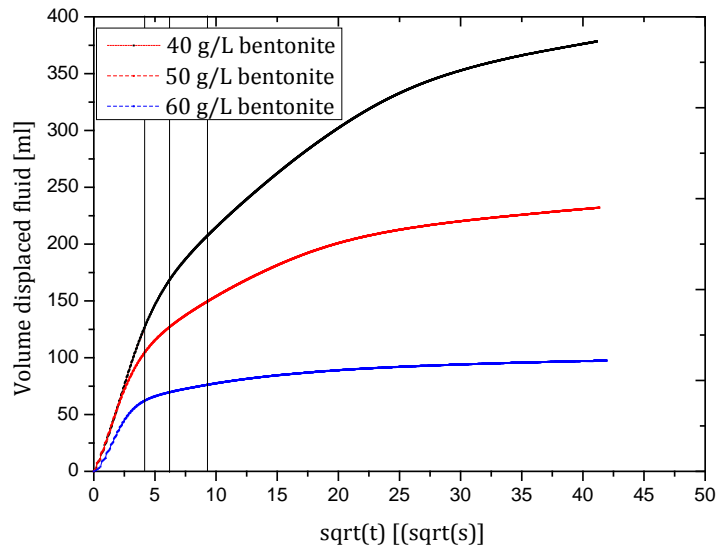


Figure 4: Measured volume displaced fluid in the infiltration tests.

Table 3: Measured and calculated parameters for each test

Bentonite content	$V_{pm}$	$h_{pw}$	$a$	$x_{max}$
g/L	ml	mm	s	mm
40	397	198	24.6	153
50	233	116	13.7	85
60	98	49	7.4	46

The distance of displaced pore water in the infiltration column is calculated as:

$$h_{pw} = \frac{V_{pw}}{A_{IC}n} \quad (8)$$

where:  $h_{pw}$  = the height of displaced pore water in the column (mm);  $V_{pw}$  = the volume of displaced fluid ( $\text{mm}^3$ );  $A_{IC}$  = the surface of infiltration column ( $\text{mm}^2$ ); and  $n$  the porosity (Krause, 1987).

It is seen from Figure 5 that the slurry infiltration depth is in order of 40 ~ 50 mm, 70 ~ 80 mm and 100 ~ 110 mm after approximately 10 seconds, 40 seconds and 80 seconds in 6, 5 and 4 g/L bentonite test, respectively.

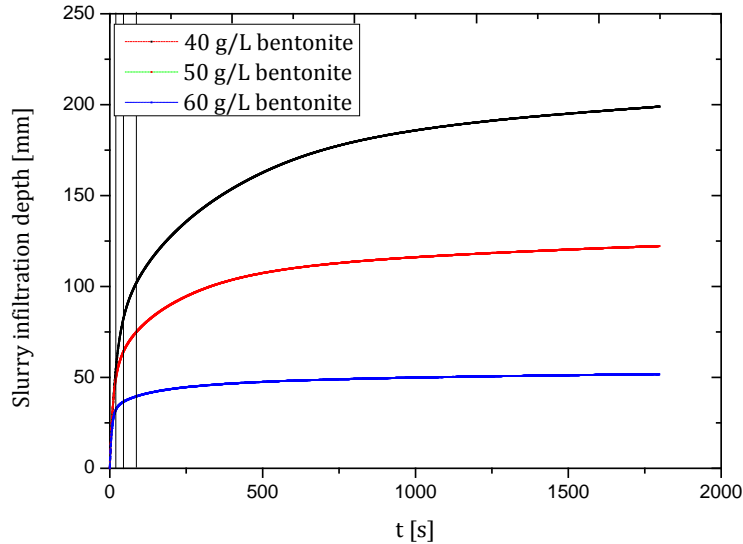


Figure 5: Measured infiltration depth in the infiltration tests.

#### 4.2. FIT OF THE SLURRY INFILTRATION FORMULAS ON THE LABORATORY RESULTS

The test results are used as a starting point in fitting the slurry infiltration formulas. The slurry infiltration depth from the laboratory tests and the fit from Broere (2001) are presented in Figure 6. The formula of Broere fit the measured infiltration depth better in tests using 50 and 60 g/L bentonite than in 40 g/L bentonite test. Due to the fact that Eq. (1) to (3) all consist of minimum of one parameter that is directly related to column infiltration tests it seems difficult to give a decent estimation of the slurry infiltration depth without conducting column infiltration tests in the laboratory.

The slurry infiltration velocity is calculated by taking the derivative of Eq. (1) with respect to time, resulting in:

$$v_{slurry} = \frac{dx}{dt} = \frac{a}{(a+t)^2} X_{max} \quad (9)$$

Note that for  $t=0$   $v_{slurry}=L_s/a$  and this value is equal to the value for  $t=0$  and  $x=0$  in equation (7).

The slurry infiltration velocity in time for both the laboratory results and equation (8) are plotted in Figure 7. The formulas of Broere show a good fit in 60 g/L bentonite test. But in 40 g/L bentonite test the infiltration velocity is overestimated in the first 27.5 seconds and the infiltration velocity in 50 g/L bentonite test is overestimated in the first 11 seconds.

Overall, the formulas of Krause and Broere can fit the laboratory results well, especially in the infiltration tests using 50 and 60 g/L bentonite in the slurry. The laboratory results can be used as input for groundwater flow models in a TBM situation (Steeneken,2016). However, therefore it will be necessary to simulate the data with equation (6) using a numerical integration. This will be the next step in this study.

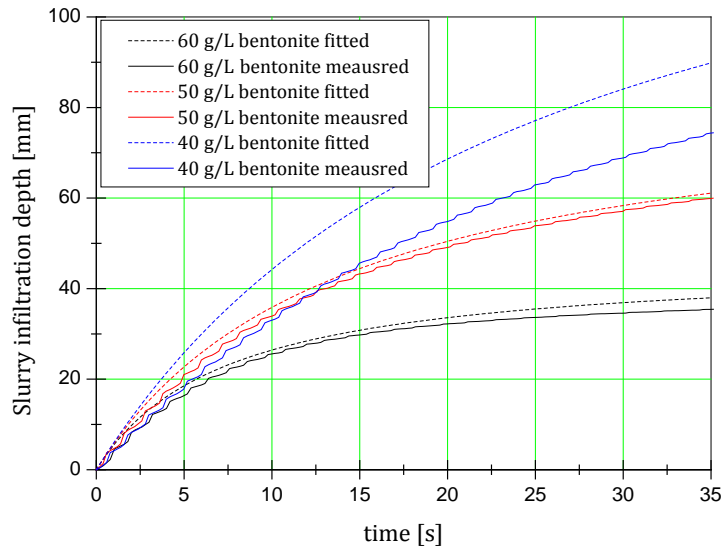


Figure 6: Fit of the slurry infiltration depth Equation (1) on the measured results.

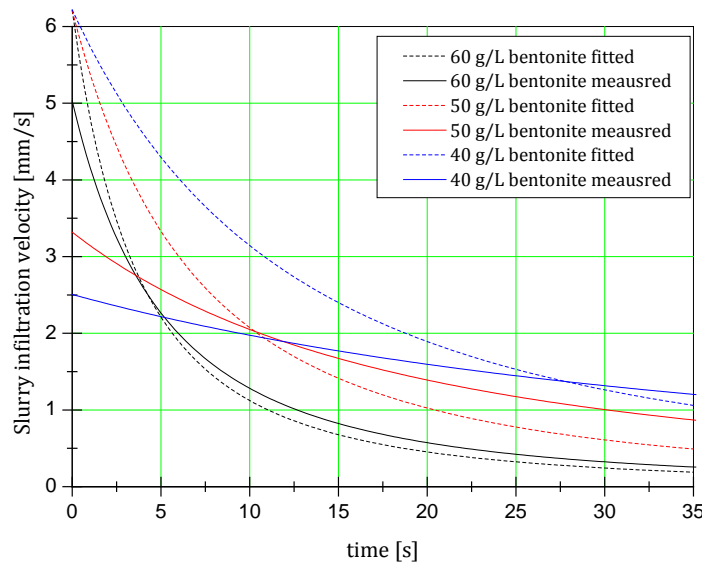


Figure 7: Fit of the slurry infiltration velocity Equation (8) on the measured results.

## 5. CONCLUSIONS

Laboratory experiments have been conducted to investigate the slurry infiltration during the TBM boring. The possible conclusions from the measurements and theory are as following:

- The slurry infiltration depth shows good resemblance with existing literature. A clear transition between slurry infiltration (mud spurt) and plastering (external filter cake formation) is distinguished.
- Remarkably, although these 2 processes can be distinguished, it appears that the resulting infiltration can be described quite well with the empirical formula of Krause (1987), that does not take into account these 2 processes.
- The slurry infiltration depth decreases with a higher bentonite percent in slurry.
- The measured infiltration velocity in beginning of the mud spurt seems higher when the bentonite concentration in slurry is higher. This is an unlikely result and needs further investigation. In the very beginning of the mud spurt the penetration velocities should be the same as is also shown in the theoretical curves of Figure 8.

- It is shown that the formulas proposed by Krause (1987) and Broere (2001) better fit the measured slurry infiltration depth and infiltration velocity for a higher bentonite concentrations in the slurry (50 g/L and 60 g/L) than for a lower bentonite concentration (40 g/L).
- Column infiltration test is recommended to predict the infiltration behaviour in slurry shield tunnel without available field data. Bezuijen et al. (2016) has shown that it is also possible with pore pressure gauges close to the TBM front to make an estimation of the slurry infiltration behaviour.
- Equation (7) takes into account the geometry of the test setup on the results. In the next phase of this research this equation will be evaluated numerically to investigate the contribution of the various terms: the permeability of the sand for water and slurry respectively, the porosity and pressure difference.

## REFERENCES

- [1] AIME R, ARISTAGHES P, AUTUORI P. and MINEC S., 2004. 15 m Diameter Tunneling under Netherlands Polders, Proc. Under-ground Space for Sustainable Urban Development (ITA Singapore), Elsevier pp. 1-8.
- [2] ANAGNOSTOU G. & KOVÁRI K., 1994. The face stability of Slurry-shield-driven Tunnels. Tunnelling and Underground Space Technology, Vol 9. No.2. pp 165-174.
- [3] BAKKER K.J. & BEZUIJEN A., 2009. 10 years of bored tunnels in the Netherlands. Proceeding 6th Int. Symposium on Under-ground Construction in soft Ground, Shanghai, 2008, CRC Press/Balkema, Leiden.
- [4] BEZUIJEN, A., STEENEKEN, RUIGROK, Monitoring and analysing pressures around a TBM, 2016. 13th International Conference Underground Construction, Prague
- [5] BEZUIJEN, A. & TALMON, A.M. 2009. Processes around a TBM. Proc. 6th Int. Symp. on Underground Construction in Soft Ground, Shanghai, 2008. CRC Press/Balkema, Leiden 3-13.
- [6] BEZUIJEN A., TALMON A.M., KAALBERG F.J. and PLUGGE R., 2004. Field measurements of grout pressures during tunneling of the Sophia Rail tunnel. Soils and Foundations vol, 44, No 1, 41-50, February
- [7] BEZUIJEN A., 2002. The influence of soil permeability on the properties of a foam mixture in a TBM. 3rd. Int. Symp. on Geotech. Aspects of Underground Construction in Soft Ground, IS-Toulouse
- [8] BEZUIJEN A., PRUIKSMA J.P., MEERTEN H.H. van 2001. Pore pressures in front of tunnel, measurements, calculations and consequences for stability of tunnel face. Proc. Int. Symp. on Modern Tunneling Science and Techn. Kyoto.
- [9] BROERE W. Tunnel Face Stability & New CPT Applications (PhD Thesis). 2001, p. 208. ISBN: 9040722153.
- [10] FESTA D. 2015, On the Interaction between a Tunnel Boring Machine and the Surrounding Soil. PhD\_thesis, Delft University of Technology.
- [11] KAALBERG F.J., DE NIJS R.E.P., and RUIGROK J.A.T. "TBM face stability & excess pore pressures in close proximity of piled bridge foundations controlled with 3D FEM". In: Geotechnical Aspects of Underground Construction in Soft Ground (2014), pp. 555-560.
- [12] KRAUSE. T. (1987) Schildvortrieb mit flüssigkeits- und erdgestützter Ortsbrust (PhD thesis) (in German).
- [13] STEENEKEN, S.P. (2016) Excess pore pressures near a slurry tunnel boring machine: Modelling and measurements. Msc-thesis, Delft University of Technology, department Civil Engineering.
- [14] TALMON A. M., MASTBERGEN D. R., and HUISMAN, M., 2013 "Invasion of pressurized clay suspensions into granular soil". In: Journal of Porous Media 16 pp. 351-365.

**PhD candidate, Tao Xu**  
**Ghent University, Ghent, Belgium**  
**E-mail address: tao.xu@ugent.be**

**Professor, Dr., Adam Bezuijen**  
**Ghent University, Ghent, Belgium and Deltares, Delft, The Netherlands**  
**E-mail address: adam.bezuijen@ugent.be**